Journal of ELECTRICAL ENGINEERING, VOL. 63, NO. 4, 2012, 201–212

REDUCING OSCILLATIONS DURING POSITIONING OF A SERVOMECHANISM HAVING FLEXIBILITY

Peter Hubinský [*] — **Peter Häuptle** [**]

This contribution describes the method of harmonic modulation of a velocity set-point signal in control to reduce undesirable oscillations. Especially the combination of this method with the well known input shaping method is of interest. Such a solution seeks for instance to a control structure used for servomechanisms equipped with a gear-box or namely mechatronic drives (MDs); where undesirable oscillations in transient- as well as semi-steady-states could arise. The combination of the methods has been proofed under real conditions in an experimental setup. Based on this, simulations regarding different industry demands and the proper choice of the modulation signal types will be introduced. Further it will be discussed which modulation signal should be used for the corresponding *ie* industrial demands. Both proposed methods are in the category of feed-forward-control which led to a practical implementation where no additional sensor (for measuring these undesirable effects) is needed to improve the system dynamics.

K e y w o r d s: oscillation, modulation, shaping, gear-box, mechatronic-drive, servo

1 INTRODUCTION

In automation it is always a challenging aim to speed a system up by having enough accuracy during positioning. In order to not exceed mechanical machine sizes, an increase in speed often causes undesirable effects like vibrations or oscillations. Especially in robotics an oscillating end-effector during a movement or also at reaching the target-position is cumbersome. In modular robotics where mechatronic drives (MDs) are used, the combination of a servo-motor together with a gear-box and also its electronics for control are fused to one module. This led to a relatively high integration level which is pleasant. The momentum of a servo-motor rises generally by its size. Thus the gear-box in robotics is generally needed to transfer the relatively high rotational speeds of a small-size motor to a higher momentum at the output shaft of the drive. Ideally the power ($P = \omega M$) would stay at the same value. The use of the combination of such small-size motors together with a gear-box, reduces the weight and size which is of interest not only in robotics. The harmonic drive ® gear-box type has the possibility to have relative high reduction-ratios (*ie*1:121) by small machine sizes which is the reason why they are often used in robotics. When having a mechatronic system (MS) where *ie*a servo-motor, harmonic drive ® gear-box and a load is used, undesirable effects can occur. They can be specified into to main groups namely transient-state effects and semi-steady-state effects. Due to the gear-box and sometimes also due to the load flexibility would last which is one mayor source for an undesirable oscillation during positioning. The proposed methods to combat undesirable oscillations are the input shaping technique (for transient-state errors) and the relatively new technique of harmonic modulation (for semi-steady-state errors) of the set-point signal. The combination of both methods and the considerations which should be made will be introduced. The proper choice of the signal types used for modulation will be discussed along simulations. An finite-impulse-response-filter or namely FIR-filter for implementing a shaper will be shown beside different ways of implementing the harmonic modulator. The main advantage of these two techniques is their feed-forward-control structure where no additional sensors in the MDs are needed unless that ones for servo-motor-control (position, velocity, motor-current).

1.1 Brief Review

The use of a harmonic drive ® gear-box may led to effects like the "kinematic-error" mentioned in [1–3]. The names origin is due to the effect which lasts generally when the gear-box causes errors in robotics. Kinematic describes the positions and poses in robotics regarding the chosen coordinate-system. Thus an error caused by the gear-box within a robotic system lasts in an error in position or kinematic respectively. Non ideal assembly of the flex-spline (a part of the harmonic drive) which led to eccentric or also named to a dedoidal condition [2] can also be a source of undesirable oscillations. Beside the gear-box, the motor and the load can also cause spectral components as *eg* torque ripples [4, 5] which lasts also in an undesirable oscillation. Modeling of a harmonic drive have been made by [6, 7]. [6] obtained further good results

[*] Slovak University of Technology in Bratislava, Slovakia, Faculty of Electrical Engineering and Information Technology, Institute of Control and Industrial Informatics, Ilkovičova 3, 812 19 Bratislava 1, peter.hubinsky@stuba.sk, [**] Heilbronn University, Germany, Faculty of Electronics and Mechanics, Max-Planck-Str. 39, 74081 Heilbronn, peter.haeuptle@hs-heilbronn.de

DOI: 10.2478/v10187-012-0030-x, ISSN 1335-3632

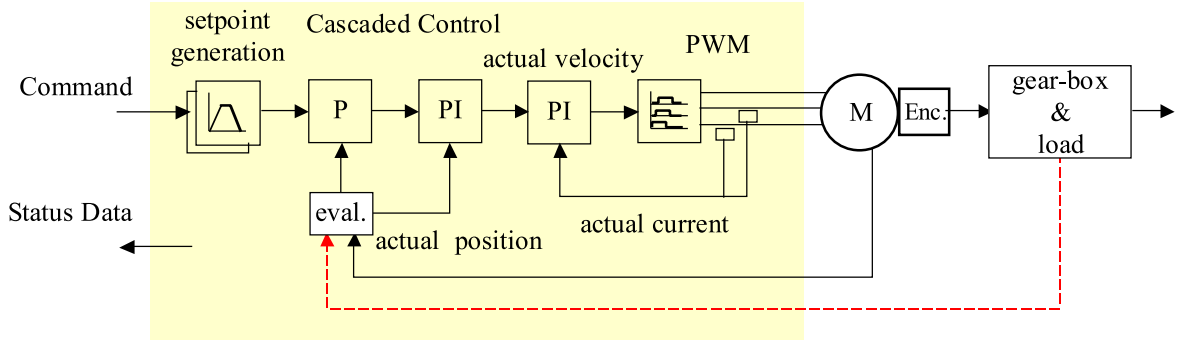

Fig. 1. MD control problem

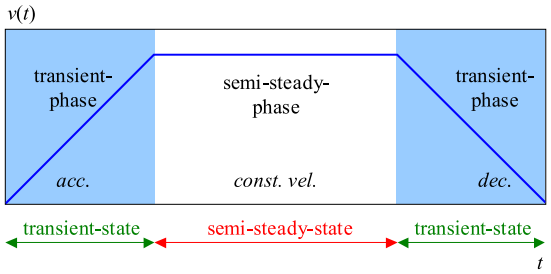

Fig. 2. Trapezoidal set-point profile

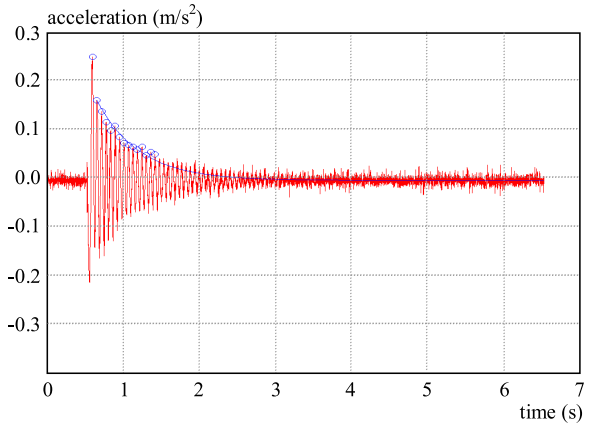

Fig. 3. Measured system "impulse"-response (time-domain)

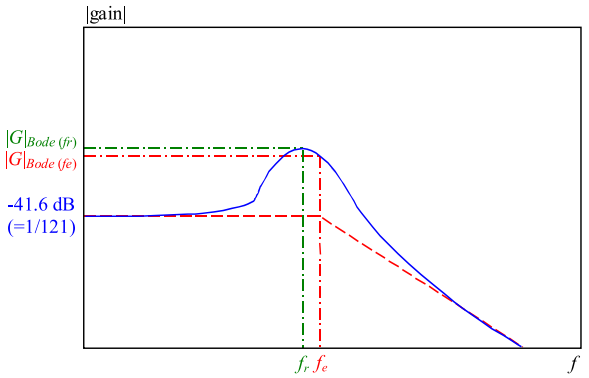

Fig. 4. Bode scheme

regarding torque control. A model summarizing the harmonic drive gear-box together with the motor and load is served by [8, 9]. As already mentioned we seek for a solution where no additional sensor is capturing the undesirable oscillation. Hence feed-forward methods are of interest. Regarding the transient-state oscillation the namely input shaping technique is known to reduce or even eliminate them. In 1957 [10] introduced the idear of modifying the input signal given to a system by using the input signal and its positive casted version to namely posicast control. With the right adjusted delay, both oscillations which would arise out of these two signals, would self-canceling each other. Later when applied for positioning the posicast control is then mostly named input shaping. In 1988, [11] extended the method (*ie* ZVD-shaper) to be less sensitive for parameter changes. Also multi-mode shapers in case of multiple transient oscillation frequencies has been developed. A lot of these applications also with modifications and different demands have been made by [12–16] regarding the field of automation. The method of harmonic modulation has been introduced the first time in June 2011 in [17] and with a slightly difference in the control structure in [18]. Different optimization methods for the signal types used for modulation were introduced in [19]. Further investigation to signal types has been also shown in [20].

1.2 Purpose of this Contribution

Within this contribution the proposed methods (shaper in combination with harmonic modulator) will be shown along the considerations which need to be made for implementation. Especially the specific demands which comes along with different applications will be stated out and discussed regarding simulations. This is important to have a proper choice for the modulation signal type in the harmonic modulator. Real measured results from an experimental setup will be shown as a proof and to judge the methods. Further different as well as new ways for implementation will be given along practical issues.

1.3 Problem Statement

The aim of any method mentioned so far is to reduce or ideally eliminate undesirable oscillations occurring in a mechatronic system. In our case a mechatronic system (MS) consists of a mechatronic drive (MD) and the load. The used MD is a servo-motor combined with a harmonic drive gear-box where the electronics and the controller are

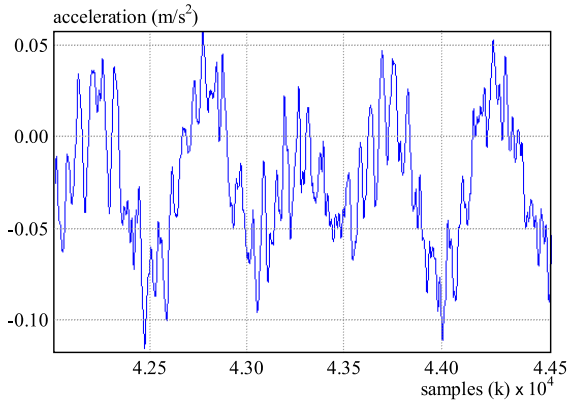

Fig. 5. Measured semi-stead-state oscillation (time-domain)

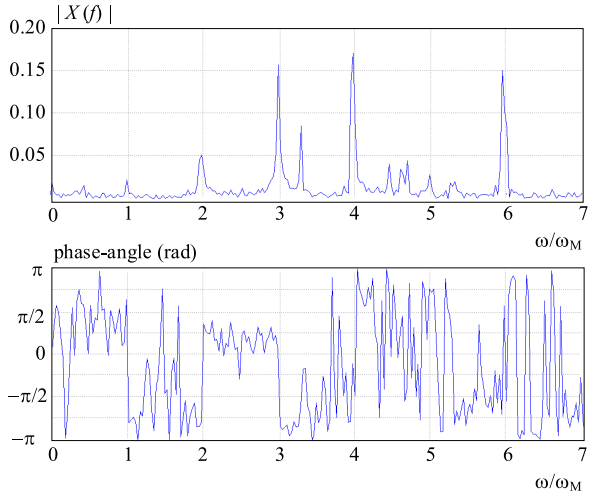

Fig. 6. Measured semi-stead-state oscillation (frequency-domain)

Table 1. System Parameters [8]

Parameter	Value	Unit
i	1/121	–
D	0.012	–
f_d	16.918	Hz
f_e	16.919	Hz
f_r	16.917	Hz

also joined with the actuator to one module. Due to the imperfect gear-box and in some cases also the load there are flexibilities in the MS which may led to undesirable oscillations. As to the fact, that only solutions regarding control are the aim, the straightforward idea would be the use of a sensor measuring these oscillations to serve the information for feedback control.

In Fig. 1, a standard cascaded control structure is shown, where the dashed (red) line shows the wished feedback of the actual value. The problem is, that a solution with an additional sensor is not worthwhile due to the following reasons:

- Constructional issues: size & weight of the sensor, wiring via brushed contact rings
- Costs
- *Existence of suitable feed-forward solutions*

In [8, 9] it is already shown, that for a mechatronic system like the used experimental setup there are two different origins for oscillations.

In Fig. 2, a commonly used set-point profile for a basic movement, namely trapezoidal-velocity profile, is shown. During acceleration and deceleration phases namely the transient-phase, the transient oscillation will be excited. Depending on the system damping, the transient oscillation lasts longer than the actual transient-phase. Thus, the time-range where the transient oscillation occurs is *ie*named transient-state.
In case of not the transient-state but moving with a constant velocity (*semi-steady phase*) we have the situation of namely semi-steady-state. Within semi-steady-state there is also a oscillation of the MS due to the kinematic-error and others.

1.4 Transient-State Oscillation

In Fig. 3 the measured transient oscillation occurring by a very small impulse as set-point signal is shown. In [8,9] the system got modeled to a relatively low damped oscillating system namely "P–T_2"-system ($0 < D\,(\approx 0.012) < 1/\sqrt{2}$).

In Fig. 4 the relation between the system eigen frequency (f_e) and the resonance frequency (f_r) is shown regarding the damping is of the form ($0 < D\,(\approx 0.012) < 1/\sqrt{2}$).

Then the transfer function (regarding position) of such a system can be written as [8, 9]

$$G_{(s)} = \frac{i}{1 + 2D\frac{s}{\omega_e} + \frac{s^2}{\omega_e^2}}\,, \quad D < 1/\sqrt{2} \tag{1}$$

where $i = 1/121$ is the specific gear-ratio of the harmonic drive gear-box which is known and the s indicates the complex variable domain. The ω_e is the angular eigen frequency or also natural frequency. This can be obtained by the use of the following relation [21, 22].

$$\omega_d = \omega_e\sqrt{1 - D^2} \iff \omega_e = \frac{\omega_d}{\sqrt{1 - D^2}} \tag{2}$$

where ω_d is the angular frequency of the damped oscillating system. In addition the resonance frequency (f_r or it's angular representation ω_r) is also of deeper interest which can be determined due to [21, 22]

$$\omega_r = \omega_e\sqrt{1 - 2\cdot D^2} \quad \text{for } D < \frac{1}{\sqrt{2}}\,. \tag{3}$$

This is already illustrated in the Bode scheme in Fig. 4, where we might see, that the maximum gain (resonance) occurs when the input signal has the same frequency equal to the resonance frequency. With the used experimental setup the values stated out in Table 1 could be obtained from modeling.

N o t e . The proposed feedforward method to reduce this kind of an undesirable oscillation is the input shaping technique.

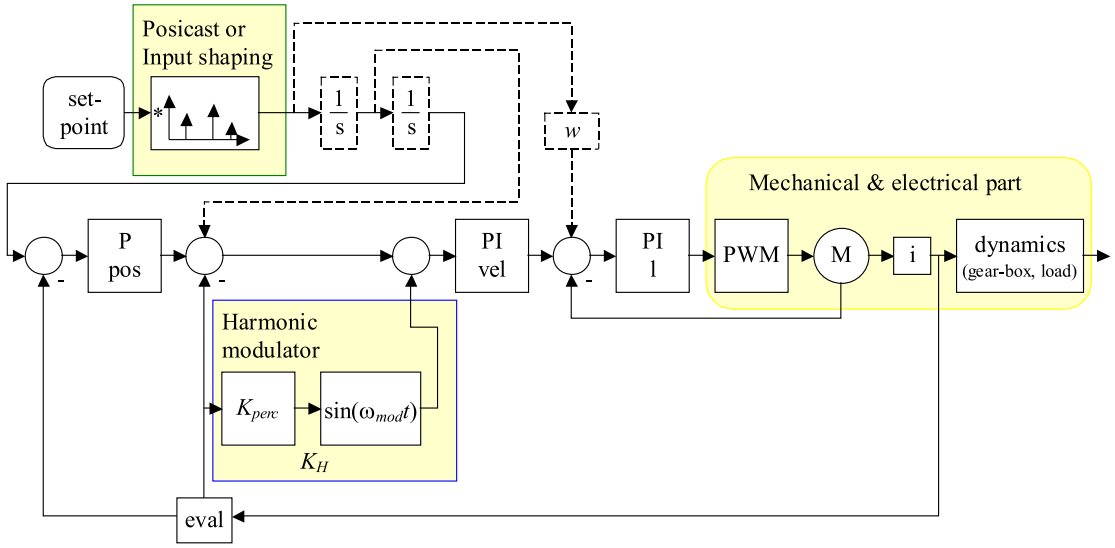

Fig. 7. Control Structure [18]

1.5 Semi-Steady-State Oscillation

Based on the experimental setup in Fig. 5 the measured time domain signal of a semi-steady-state oscillation is shown [8, 9].

Figure 6 shows the respective frequency domain information (single sided amplitude spectrum).

In a pure linear system there would no undesirable oscillation occur during the phase (see add. Fig. 2) of moving with a constant velocity. Constant velocity is a so said steady-state because no transient condition *eg* acceleration is occurring. Due to the fact that the system is moving we introduced the specific name semi-steady-state. The latest empirical model has been developed in [9]. For this contribution it is not of interest working with an empirical model because then the proposed method is not comparable for other applications than our used setup. Thus it will be shown later, that we can even show the advantage of the harmonic modulator using in simulation the linear transfer function in (2), which will cover a more widespread range of applications. In addition this would allow us to say that the method will work generally.

N o t e . The proposed feedforward method to reduce this kind of an undesirable oscillation is the harmonic modulation of the velocity set-point signal.

1.6 Control Structure

In [18], the proposed control structure in Fig. 7 has been introduced the first time.

The set-point signal is generated by the use of trapezoidal trajectories as indicated in Fig. 2. The left and right blocks with the shaper modifies the set-point signal to suppress the transient oscillation. The "$1/s$"-blocks indicates numerical integration. This, together with the dashed lines is only needed if map-based pilot control is wished. The w is then only a conversion factor to bring the acceleration- to a current-signal. A three stage cascaded control is used, where position, velocity and motor current is controlled. There is to say that an incremental encoder mounted on the motor-shaft is used to determine the position and velocity of the drive. The right highlighted block indicates the mechanical and electrical part where the servo-motor is driven by a pulse-width-modulated signal. The gear-ratio i reduces the speed by increasing the momentum. The dynamics of the gear-box are not specifically measured as already mentioned. The bottom highlighted block indicates the harmonic modulator. Depending on the actual speed as well as the given percentage in K_{perc}, the gain K_h for the amplitude of the modulated signal is generated. That is a single sine signal for modulation is applied whose frequency is stated out in ω_{mod}. The harmonic modulator can also be placed before or after the shaper (like introduced in [17]).

2 THEORY

Within this section all theory parts will be handled. The proposed methods harmonic modulation as well as the input-shaping will be shown and new ways of implementation regarding digital discrete systems will be introduced. In addition some simulations are shown which will be discussed later.

2.1 Harmonic Modulation

When keeping in mind Fig. 7 then the harmonic modulator for a single sine signal can be stated out to

$$Out = -K_h \sin(2\pi f_{mod} t) = -K_h \sin(\omega_{mod} t) \qquad (4)$$

and

$$K_h = K_{perc}(\dot{\varphi}_M i) \qquad (5)$$

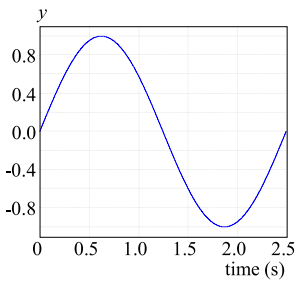

Fig. 8. Sine-signal

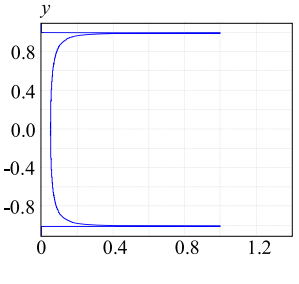

Fig. 9. Histogram of sine-signal

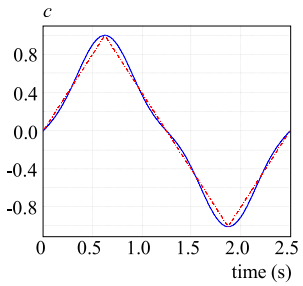

Fig. 10. Second order triangle-signal; $a_f = 0.157$

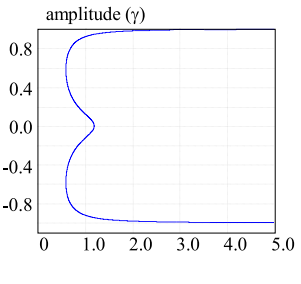

Fig. 11. Histogram of 2nd order triangle signal; $a_f = 0.157$

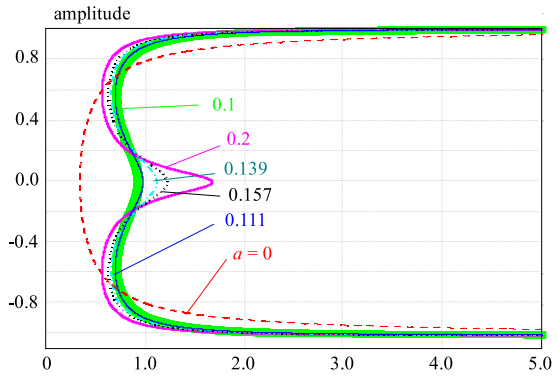

Fig. 12. Histogram of 2nd order triangle; different a_f's

Table 2. Optimization results [19]

Optimizing method	ampl. ratio	value
min hist-domain	$a_f = min_h$	$= 0.105$
min quad. hist-domain	$a_f = min_{h^2}$	$= 0.205$
min time-domain	$a_f = min_t$	$\cong 0.139$
min quad. time-domain	$a_f = min_{t^2}$	$\cong 0.157$
hist at zero ampl.	$a_f = \frac{\pi-2}{3\pi+2}$	$\cong 0.1$
quad. hist at zero ampl.	$a_f = \frac{2\pi-2}{6\pi+2}$	$\cong 0.2$
Fourier:	$a_f = a_{f\,\text{fourier}}$	$= 0.\overline{111}$

where we might see, that the amplitude gain K_h is due to K_{perc} always relative to the actual velocity of the servo-motor ($\dot{\varphi}_M$). The i is the specific gear-ratio *ie* 1:121.

N o t e . So far f_{mod} is always constant.

In case of a multi sine signal the following can be written

$$\begin{aligned} Out &= K_h \sum^{n} K_{hn} \sin(2\pi n f_0 t) \\ &= K_h \sum^{n} K_{hn} \sin(n\omega_0 t) \end{aligned} \tag{6}$$

where f_0 is the the first harmonic or the lowest frequency content. The n indicates the nth harmonics of f_0. The K_{hn} is an additional weight to adjust the specific gain for each harmonic.

2.2 Signal-types for Modulation

In [20] different signal types for the use in a harmonic modulator has been investigated. The most interesting two of them will be mentioned below which is needed for further investigation or simulation respectively. Beside the signal in time-domain also the histogram or namely hist-domain is important. The more histogram is uniformly distributed, the better regarding transient-effects [20].

2.2.1 Sine signal

The sine signal, see also (16), offers good performance and is relatively easy to implement [20].

In Fig. 9 we may see that the histogram is not uniformly distributed like when having *eg* triangle signal, the dashed, (red) curve in Fig. 10. The triangle signal itself does have higher harmonics or higher frequency contest respectively. This may arise a transient oscillation which is not of interest; although the hist-domain is "ideal".

2.2.2 2nd order triangle signal

The 2nd order triangle signal, see also (18), is a compromise between the "ideally hist-domain" triangle signal and having only a few harmonics (*ie* 2, thus 2nd order) [20].

In Fig. 11 we may see that the hist-domain of the 2nd order triangle signal is compared to Fig. 9 closer to the uniformly distributed case. As already mentioned the 2nd order means that two different harmonics are used to build up that signal *ie* the first and the third harmonics. Then the question is what might be a good fitting ratio between the amplitudes of these two frequency contents should be used (see also (18)). This ratio is named "a_f" and in [19] different ways of obtaining an optimum setting for a_f has been analytically developed. Later some new practical simulations will be introduced and discussed. The histograms lasts to Table. 2 and are plotted in Fig. 12.

Table 2 summarizes the results of the different optimization techniques used in [19]. The last row is an additional case to be comparable with the Fourier inter-

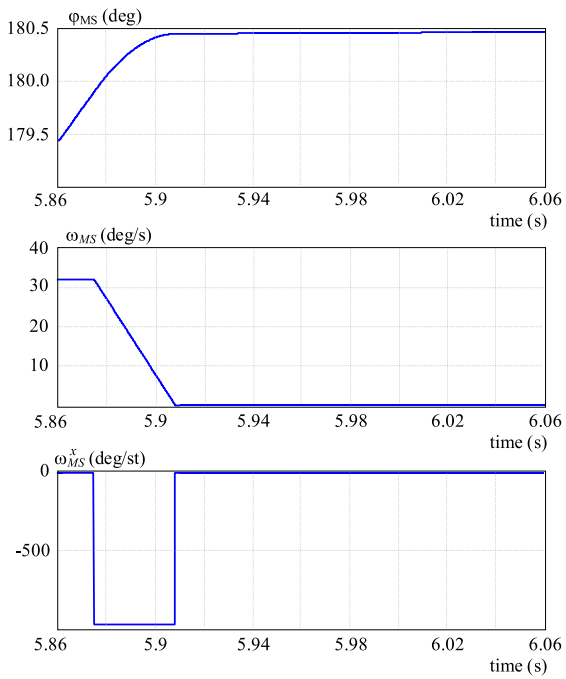

Fig. 13. Desired signal without shaping example

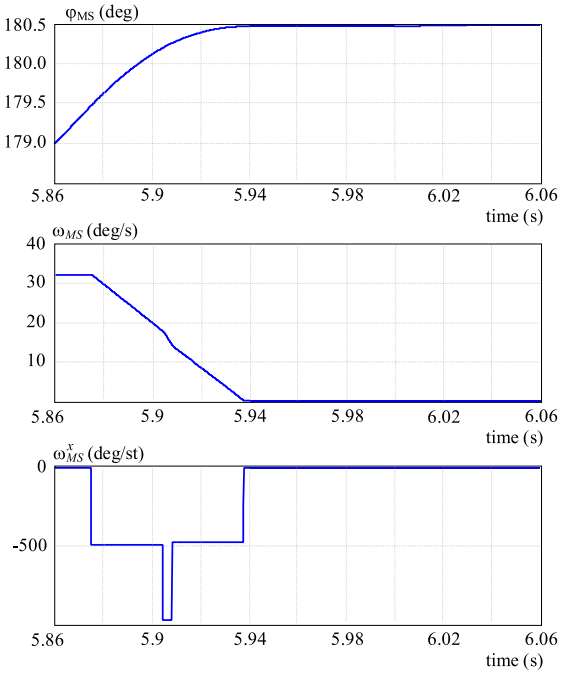

Fig. 14. Desired signal of a ZV-shaping example

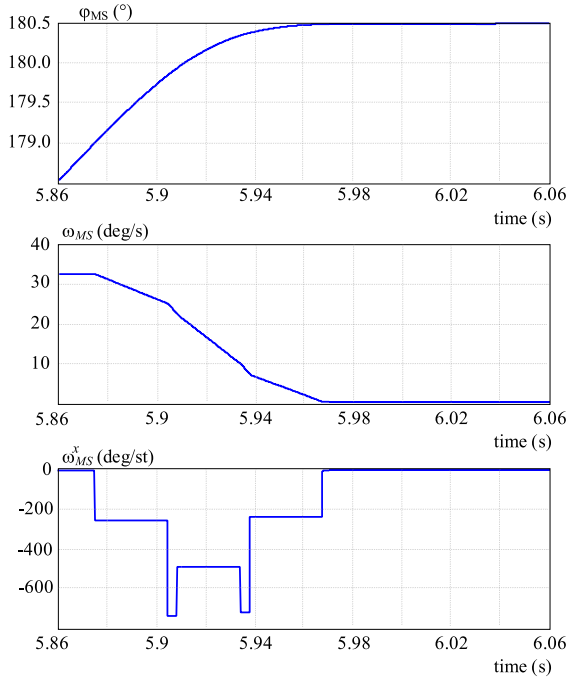

Fig. 15. Desired signal of a ZVD-shaping example

pretation cut after the 3rd harmonic. So in general the optimum values for a_f could be limited to [19]

$$0.1 \leq a_f \leq 0.2\,. \tag{7}$$

Later new simulations will use these results from Table 2.

2.2.3 Discrete Implementation

Generally, there is to mention that with respect to Fig. 8 as well as Fig. 10 we have only "odd" function types which means that only odd harmonics are existing. This simplifies the implementation in the following way: To obtain the signal over the full period we need actually only focus to the first quarter of a period. When having the first quarter $(0 \leq t < T/4)$ then the second quarter $(T/4 \leq t < T/2)$ can actually be vertically mirrored (due to "axial-symmetry") at $t = T/4$. Up to now the first half period is ready $(0 \leq t < T/2)$. The second half period $(T/2 \leq t < T)$ can then again be mirrored horizontally (due to "point-symmetry") from the first half period. Thus we may say, that knowing the first quarter period of an odd function is enough to implement the full period of such a function.

In a discrete system there are in most cases two different kind of efforts when implementing an algorithm. Either the algorithm takes more efforts in calculation time or it takes more efforts in consuming memory.

In most discrete system like microcontrollers, PLCs, *etc* the operations: adding, subtracting, multiplying, dividing and modulo are basically supported. The use of a sine, cosine or tangential operator are mostly causing more efforts in such a device. For our demands we need to focus on the sine function which is used in both signal types (sine, 2nd order triangle). One way to calculate the sine in a discrete system is to use the supported already coded library. Second possibility would be the use of a "look-up-table". Regarding on the resolution chosen (*eg* 16bit) the interval $0 \leq t < T/4$ is divided by (*eg* 65535 @ 16bit) steps and stored in memory. So to each interval

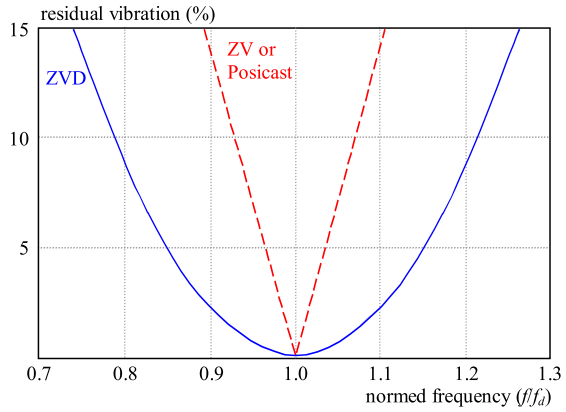

Fig. 16. Sensitive graphs of diffrenet shaper types

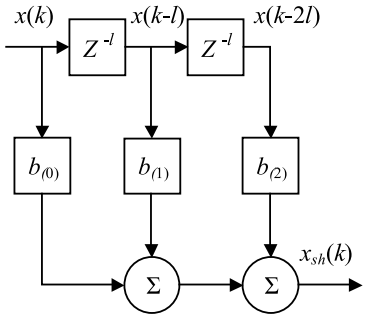

Fig. 17. FIR for a ZVD-shaper with three coefficients (i.e. b_0 to b_2) in discrete time

step the respective value is stored in memory. A third alternative would be the use of a "Taylor-approximation" especially for that interval $0 \leq t < T/4$. Roughly spoken: The Taylor-approximation is a polynomial approximation *ie* of the sine signal. For a specific interval a finite polynomial function exists which is very close to the "pure" sine function. The Taylor-series is defined as [23]

$$\sum_{m=0}^{\infty} \frac{f^{(m)}(b)}{m!}(t-b)^m \tag{8}$$

where b (*ie* $b = 0$) is the seeding value around the series will be build up. The $f^{(m)}$ is the mth derivation of the specific function (*ie* sine). The solution especially for the sine function can be written to [23]

$$\sin(t) = \sum_{m=0}^{\infty} \frac{(-1)^m}{(2m+1)!} t^{2m+1} = t - \frac{t^3}{3!} + \frac{t^5}{5!} - \dots \tag{9}$$

An approximation would be a value for ($m \ll \infty$). Note: The value $b = 0$ is good fitting because for small values of t the $\sin(t) \approx t$ which affects good as a linear approximation. Otherwise the middle of the interval of interest (*ie* $b = T/8;\ 0 \leq t < T/4$) would be the right choice.

2.3 Input-Shaping

Regarding the case when using posicast-control for shaping the set-point signal for positioning system and the investigation in [15] are the basis for the following two shaper types. We just want to show the ZV-shaper beside the ZVD-shaper. When considering a movement where the trapezoidal velocity profile is used (see also Fig. 2) then the acceleration or deceleration phase is of interest. In Fig. 13 we can the set-point signal during the deceleration phase of a movement. The upper plot shows the position over time, the plot in the middle the velocity over time and the lower plot the acceleration over time.

N o t e . In Fig. 13 no shaping is applied.

2.3.1 Zero Vibration

The ZV-shaper would change the set-point signal for example to that one shown in Fig. 14. The only parameters need to be known to set the shaper properly are the system eigen frequency (f_e) as well as the damping (D).

The shaping might be very good visible when having a look to the acceleration signal in Fig. 14 compared to Fig. 13. We might also see, that the duration of the movement is slightly increased. This is the cost of using a shaper to reduce or even eliminate an undesirable transient oscillation [15].

2.3.2 Zero Vibration and Derivative

The ZVD-shaper does also need the two parameters f_e and D and lasts for example to Fig. 15.

Compared to Fig. 14 the duration of the movement is again slightly increased. This is the cost of being less sensitive to parameter changes like shown in Fig. 16 [15].

Figure 16 shows that when having a linear system and the shapers are set properly ($f/f_d = 1$) then both shapers are completely eliminating the undesirable transient oscillation. This means no residual vibration of the system is lasting. If the shapers are not set properly *eg* when $f/f_d = 0.9$, then the ZVD-shaper offers a better performance compared to the ZV-shaper, thus less sensitive. Note: f_e is the system eigen frequency or natural frequency which is a fundamental information of a linear system. The f_d is the damped frequency oscillation which lasts at the system output (see also (2)).

2.3.3 Discrete Implementation

The discrete structure which can be used to implement both types of shapers is shown in Fig. 17. The figure shows a Finite-Impulse-Response filter (*FIR-filter*) which can also be seen as a taped-delay filter comparable to a First-In-First-Out buffer (*FIFO-buffer*) with weighted factors. The big advantage of a FIR-filter is that they are always stable in their behavior.

The z in Fig. 17 indicates the discrete time. Thus the block with z^{-l} is actually a time delay of $t = l \cdot T_s$ where

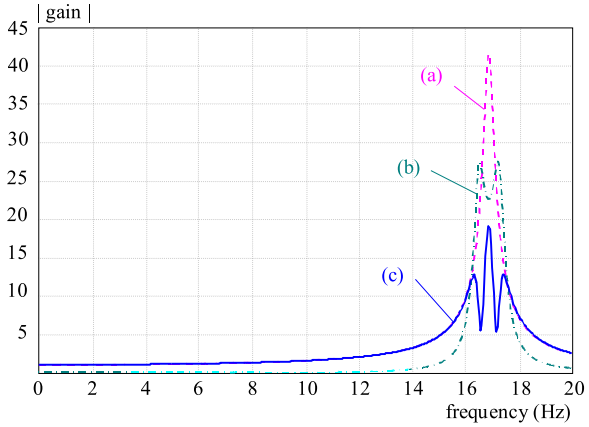

Fig. 18. Simulation of sine; $K_{perc} = 8\%$, $f_{mod} = 0.4\,Hz$; (a) – P–T$_2$ system, (b) – transfer behavior of the modulator, (c) – the whole system behavior

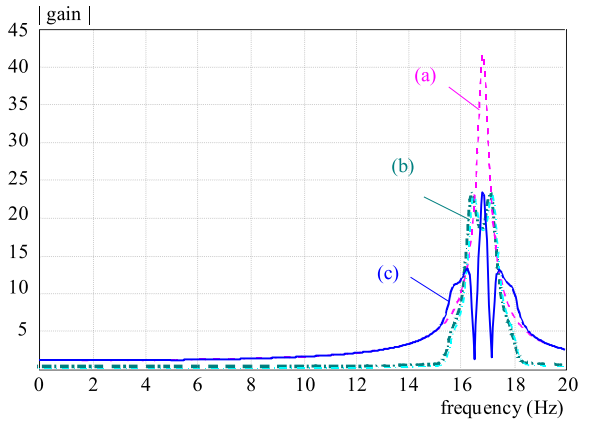

Fig. 19. Simulations of 2nd order triangle; $a_f = 0.157$, $K_{perc} = 8\%$, $f_{mod} = 0.4\,Hz$; (a) – P–T$_2$ system, (b) – transfer behavior of the modulator, (c) – the whole system behavior

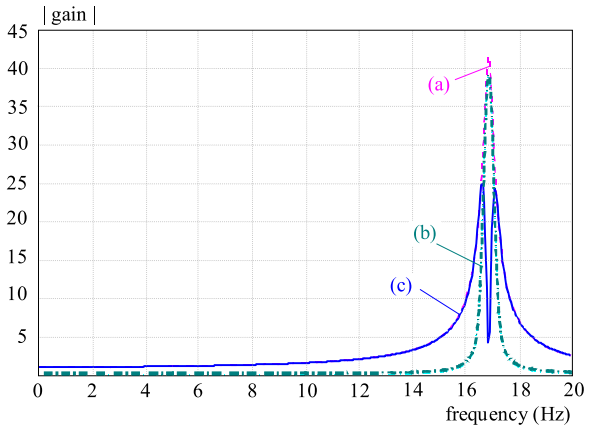

Fig. 20. Simulatioin of 2nd order triangle; $a_f = 0.157$, $K_{perc} = 20\%$, $f_{mod} = 0.1\,Hz$; (a) – P–T$_2$ system, (b) – transfer behavior of the modulator, (c) – the whole system behavior

l must be an integer. The T_s is then the respective sampling time used in the system. The b_0, b_1 and b_2 are weighting factors. Where b_2 is just used when implementing the ZVD-shaper. In case of the ZV-shaper, b_2 can be set to zero or just neglected. The question now lasting is how to get proper values for l, T_s, b_0, b_1 and (if needed) b_2. Generally due to [10]

$$lT_s = \frac{2}{f_e} \tag{10}$$

where in some cases there is a difficulty to force l to an integer. To find a proper choice regarding T_s in [24, 25] are possible proposals published. If T_s is already fixed and the error due to the rounding error which would arise when satisfying (10) is too large, in [15] a method is introduced where b_1 is split into two factors *eg* to $b_{1,1}$ and $b_{1,2}$ with a relatively short time delay in between. In case of the ZVD-shaper also b_2 might also be split to $b_{2,1}$ and $b_{2,2}$ respectively. Regarding the ZV-shaper the following two relations can be written [15]

$$b_0 = \frac{1}{1+\alpha}, \qquad b_1 = \frac{\alpha}{1+\alpha} \tag{11}$$

and

$$\alpha = e^{-\frac{D\pi}{\sqrt{1-D^2}}} \tag{12}$$

where e is the euler number and D the damping of the system (see add. (1)). Regarding the ZVD-shaper and with respect to (12) we may write [15]

$$b_0 = \frac{1}{(1+\alpha)^2}, \quad b_1 = \frac{2\alpha}{(1+\alpha)^2}, \quad b_2 = \frac{\alpha^2}{(1+\alpha)^2}. \tag{13}$$

2.4 Basis for Simulations

The use of Bode plots showed very good visualizations, especially when using linear scaled axis instead of the normally logarithmic scaling. The absolute gain is of major interest. Roughly spoken: The Bode plot for the absolute gain can practically be obtained by feeding the system with a "chirp" sine signal. This means a sine signal whose frequency starts at 0 Hz and will be increased step by step up to the wished end of the graph. Important is, that the increase of the frequency is slow enough that the system has no transient-effects anymore. By doing so in every step, the specific output gain of the investigated system is plotted. Thus, this will last to the Bode plot for the absolute gain.

Simulations to judge the performance of the harmonic modulation are needed. Hence, in the following steps the theory on which the regarding simulations are based on, will be introduced. Due to linearity where superimposing is allowed, the system impulse response $g_{(t)}$ ($g_{(t)} = \mathfrak{L}^{-1}\{G\}$) together with the modulation signal $y(t)$ and the gain of the harmonic modulator K_h led to the following equation

$$\left[\mathfrak{L}\{g(t)\} + K_h \mathfrak{L}\{y(t)g(t)\}\right]_{(s\to j\omega)} = G_{all_{(j\omega)}} \tag{14}$$

where the "overall" transfer function is G_{all} and $\mathfrak{L}$ indicates the Laplace transformation.

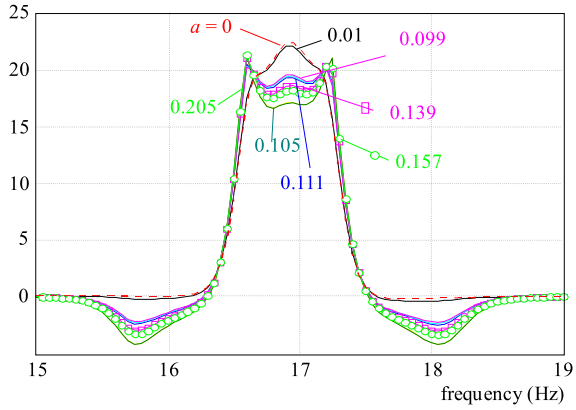

Fig. 21. Simulation 2nd order triangle with diff. a_f's; $K_{perc} = 8\%$, $f_{mod} = 0.4\,Hz$

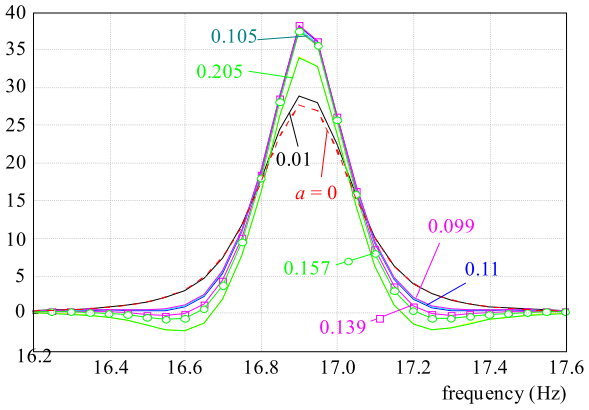

Fig. 22. Simulation 2nd order triangle with diff. a_f's; $K_{perc} = 20\%$, $f_{mod} = 0.1\,Hz$

Let us further keep in mind the Euler-form of a sine signal like applied here

$$\begin{aligned} \sin(\omega_{mod}t) &= \frac{1}{2j}\left(e^{j\omega_{mod}t} - e^{-j\omega_{mod}t}\right) \\ -\sin(\omega_{mod}t) &= \frac{1}{2j}\left(e^{-j\omega_{mod}t} - e^{j\omega_{mod}t}\right) \end{aligned} \tag{15}$$

where j indicates complex unit and ω_{mod} indicates the modulation frequency. For a modulation signal like shown in Fig. 7 and with respect to (6) where a sine signal is used we can state out

$$y_{(t)} = -K_h \sin(\omega_{mod}\, t)\,. \tag{16}$$

Then the system transfer function G (see (1)) can be combined with the respective transfer function of the harmonic modulator and additionally with respect to (4) we may write

$$\begin{aligned} G_{all_{(j\omega)}} &= G(j\omega) + K_h \frac{1}{j2} \\ &\quad \times \left[G(j\omega - j\omega_{mod}) - G(j\omega + j\omega_{mod})\right]\,. \end{aligned} \tag{17}$$

For a modulation signal containing multiple sine signals ($ie\, n = 1,\, 3$) and with respect to (6) we can further state

$$y_{(t)} = -\frac{K_h}{1 + a_f}\left[\sin(\omega_{mod}t) - a_f \sin(3\omega_{mod}t)\right]\,. \tag{18}$$

Regarding the simulation with bode we can state out

$$\begin{aligned} G_{all_{(j\omega)}} &= G_{(j\omega)} + \Gamma_{(j\omega,\, n=1)} - a_f \Gamma_{(j\omega,\, n=3)}\,. \\ \omega_{mod,\, n} &= n\omega_0\,, \quad n = 1,\, 3\,, \\ \Gamma_{(j\omega,\, n)} &= -\frac{K_h}{c_{\max}} \frac{1}{2j}\left[G\big(j(\omega + n\omega_0)\big) - G\big(j(\omega - n\omega_0)\big)\right] \end{aligned} \tag{19}$$

where the multiplication by $1/c_{\max}$ is just a norm to fit the maximum (amplitude) value ($c_{\max}$, $c_{\min}$) to ± 1. The subscript *mod* of $j\omega_{mod}$ indicates the modulation frequency and ω_0 its first harmonic. The $j\omega$ is the argument of the function.

With respect to (17) and applying to (19) we can now simulate the "overall" system for investigation.

remarkRemark The simulation technique via bode doesn't match exactly the used harmonic modulation in the experimental setup or (4) respectively (see additionally Fig. 7). In the sense of creating bode plots we do not have the information of the actual or set-point motor speed ω_M over $j\omega$. Never the less, by using the angular system frequency ω (available at bode) which may correlate with ω_M should allow us to use this instead. This has been verified in [17, 18, 20].

2.5 Simulations

Figures 18–20 show the bode plots with different settings. All of them are in both axis linear scaled instead of logarithmic due to a better visualization. The dashed (a) curves are indicating the P–T_2 system from (1). The dashed-dotted (b) curves are indicating the respective transfer behavior of just the modulator. The solid (3) curves graphs are then the overall system behavior where harmonic modulation is applied.

In Fig. 18 the case of using just the sine signal type for harmonic modulation is shown. Fig. 19 shows the use of a 2nd order triangle signal.

In Fig. 20 the same signal type is used but the modulation frequency has been reduced from $f_{mod} = 0.4\,Hz$ to $f_{mod} = 0.1\,Hz$ and the gain has been increased from $K_{perc} = 8\%$ to $K_{perc} = 20\%$.

Due to the last two figures we might see, that when changing the modulation frequency a change horizontally (X-axis, frq.) can be recognized. The higher f_{mod} the more "wider" is the dashed-dotted curve and therefore the solid curve. A change in gain would last in changes on the Y-axis (—gain—). Moreover we can see that although the same signal type is applied the shape changes when comparing Fig. 19 with Fig. 20.

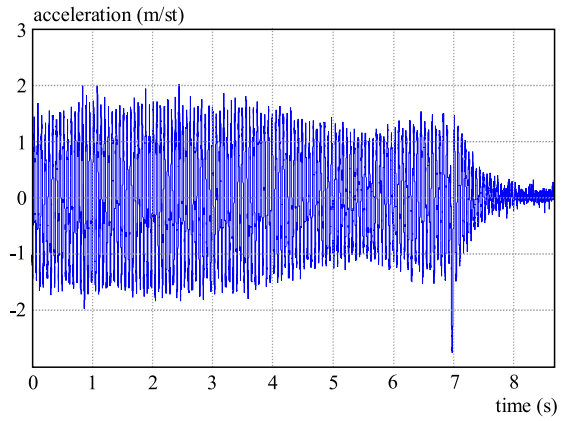

Fig. 23. Movement though 180 deg at max. 16 deg/s — without shaper & harmonic mod

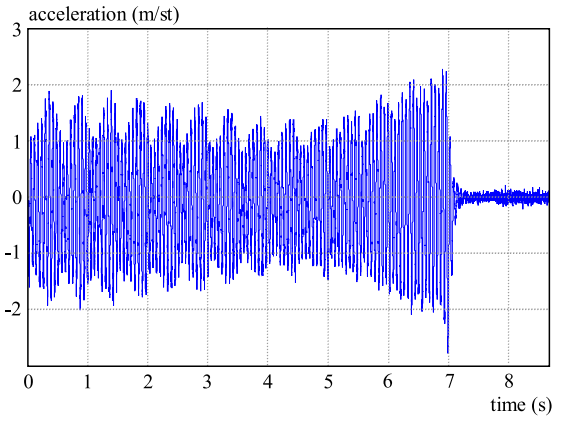

Fig. 24. Movement though 180 deg at max. 16 deg/s – with shaper & with harmonic mod; $K_{perc} = 10\%$ $f_{mod} = 2\,Hz$

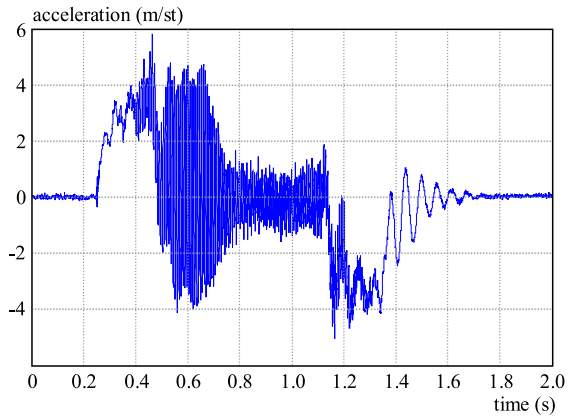

Fig. 25. Movement though 180 deg at max. 204 deg/s – without shaper & harmonic mod

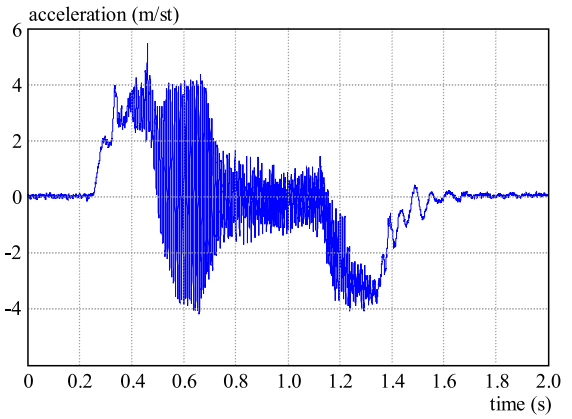

Fig. 26. Movement though 180 deg at max. 204 deg/s – with shaper & with harmonic mod.; $K_{perc} = 8\%$ $f_{mod} = 0.4\,Hz$

With respect to Table 2 and the results from [19] a more deeper investigation should be made. Therefore Figs. 21 and 22 are shown. Both figures show the effect of changing $K_{perc} = 8\%$ and $f_{mod} = 0.4$ Hz, Fig. 21, to $K_{perc} = 20\%$ and $f_{mod} = 0.1$ Hz, Fig. 22. Additionally there is to say that the graphs in these two figures has been obtained by subtracting the P–T_2 system transfer function (1) and dashed in Fig. 20, by the overall system transfer function (19) and solid in Fig. 20. In our focused region of interest ("the resonance zone"; $15 \ldots 19\,Hz$) this might be a good and valid method. This makes it easy to judge the performance. Hence, the higher the values above zero in Y-direction the better. Everything below zero in Y-direction is worse.

By comparing Fig. 21 with Fig. 22 we can see that generally the better performance is shown in Fig. 22 where the lower modulation frequency and the higher gain is used ($K_{perc} = 20\%$, $f_{mod} = 0.1\,Hz$). The higher f_{mod} in Fig. 21 needs to reduce the gain to make the performance not worse. Additionally at 15.7 Hz and 18 Hz the performance is lower compared to Fig. 22. Regarding the right choice for a_f we can state that $a_f \approx 0.1$ might be the best choice for any settings of f_{mod} or K_{perc}.

3 EXPERIMENTS

In Figs. 23 and 24 the drive moves with a constant velocity of 16 deg/s (output-shaft, not motor-shaft) over a distance of 180 deg. The full movement could not be captured due to data acquisition limits. After the time of 7 seconds we just see the lasting transient oscillation and before just the semi-steady oscillation. In Fig. 23 no input-shaping as well as no harmonic modulating is applied.

In Fig. 24 a ZV-shaper is used as well as the harmonic modulation with a sine signal type is applied.

When comparing Fig. 23 with Fig. 24 we can clearly see the almost elimination of the transient oscillation. During semi-stead-state the envelop of the modulated sine might be visible. We might also say that the semi-steady oscillation is reduced as well (7% to 30% regarding [17, 18, 20]).

N o t e . The reason for using here especially $f_{mod} = 2\,Hz$ instead of $f_{mod} = 0.4\,Hz$ compared to the simulation in Fig. 18 is for better visualization. The lower frequency ($0.4\,Hz$, $0.1\,Hz$) would make it hard to separate the envelop of the sine from the natural fluctuations

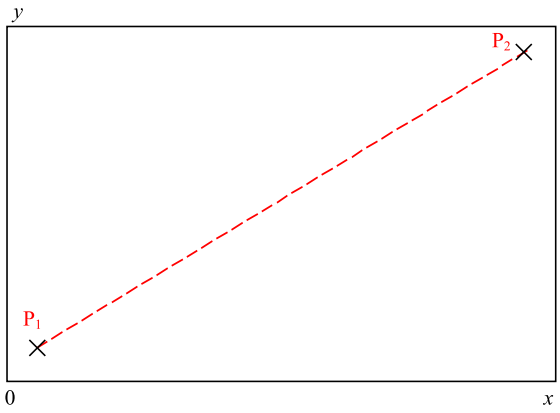

Fig. 27. Tangential velocity of XY-positioning

of the semi-steady-state oscillation. In addition there is to say that in [17, 18, 20] especially for that reason the frequency-domain was used to judge the method. The time-domain offers instead a much better visualization of the transient oscillation and has never been before published which may justify this decision. Especially the combination of both methods (shaper, modulator) is the focus in this contribution.

In Figs 25 and 26 a relatively fast movement of the drive with 204 deg/s is shown. Thus there is almost no semi-stead-phase and therefore practically no semi-steady-state. Hence the harmonic modulator wouldn't be able to serve an improvement. This kind of measurement shall specifically show if the harmonic modulator will affect the performance of the shaper. In Fig. 25 no shaper and no harmonic modulator is used. Not only but especially after the time of 1.4 seconds the transient oscillations in both figures are visible. In Fig. 26 a ZV-shaper as well as a harmonic modulator using a sine signal type is used.

When comparing Fig. 25 with Fig. 26 the shaper might not have the same almost perfect performance than in Fig. 24. Never the less a reduction is clearly visible too.

4 DISCUSSION

The measured experiments by the used experimental setup is very important to show that the proposed methods are generally working as intended. This more practically way of validating the simulated results may proof the methods. Moreover at higher moving velocities like shown in Figs. 23 and Fig. 25 it might be clear that the harmonic modulator will not make the use of a shaper dispensable. Regarding the investigation to proper values to set the harmonic modulator the following can be stated out: When using a relative low modulation frequency (f_{mod}), then higher gains (K_{perc}) in the modulator can be used to obtain a better performance in sense of reducing undesirable semi-steady-state oscillations. In many cases a higher modulation frequency would fit better due to the duration time of a movement. A movement of the drive should be at least as long as $1/f_{mod}$ (one period) where 2.5 seconds (0.4 Hz) are better than 10 (0.1 Hz). Depending on this behavior f_{mod} should be considered. In any case $a_f \approx 0.1$ is a good choice when using the 2nd order triangle signal type. This could be clearly shown by simulations.

When implementing the harmonic modulator in a discrete system and memory is not a matter, than the look-up-table technique should be used. This will last in the most fastest implementation by very less computational costs. Then only a value need to be read during runtime. When calculation power is not a manner, then the sine operation should be used directly from the respective math-library which is generally supported. A compromise when for other reasons a math-library does not want to be used or is not available, the proposed Taylor-approximation can be used. This lasts in basic math operations like multiplication, addition *etc* see (9).

5 CONCLUSION

The newly acquired measuring results in time-domain (Figs. 23–26) showed the performance of the harmonic modulator in combination with input-shaping. Especially in time-domain the performance of the shaper could be stated out more clearly than in previous publications. Generally the methods are working. The new ways of implementing the methods, can additionally reduce the computational efforts in the discrete system where they are planned to be implemented. In this contribution the full overview of both proposed methods (shaper, modulator) should be served along some practical issues like the implementation. The simulated results beside real measurements should make clear that the performance of 7% up to 30% improvement in sense of reducing any undesirable oscillation could be reasonable. Not using an additional sensor in control might be a very attractive consideration for industrial demands. Even when having a multi axis system like to linear axis, then the harmonic modulation shouldn't change the position accuracy like the Fig. 27 shows. The dashed line is showing the trajectory from position P_1 to position P_2. The closer the dashes, the higher the velocity. The line itself is straight which is the aim to held precision. Just the velocity is tangentially changing. Sure this is not desirable for all kinds of applications like welding or LASER-cutting for instance. In applications where 8% or even 20% (K_{perc}) tangential velocity changes are allowed the methods are worth to implement.

Acknowledgments

The authors would like to thank the company "SCHUNK GmbH" in Lauffen/Germany.

References

[1] GHORBEL, F. H.—GANDHI, P. S.—ALPETER, F.: On the Kinematic Error in Harmonic Drive Gears, Trans. American Society of Mechanical Eng. Journal of Mechanical Design **123** No. 1 (2001), 90–97, http://dx.doi.org/10.1115/1.1334379.

[2] EMEL'YANOV, A. F. *et al*: Calculation of the Kinematic Error of a Harmonic Gear Transmission Taking into Account the Compliance of Elements, Soviet Engineering Research **3** No. 7 (1983), 7–10.

[3] GANDHI, P. S.—GHORBEL, F. H.: Closed-Loop Compensation of Kinematic Error in Harmonic Drives for Precision Control Applications, Control Systems Technology, IEEE Transactions on **10** No. 6 (2002), 759–768.

[4] NANDI, S.—TOLIYAT, H. A.: Condition monitoring and fault diagnosis of electrical machines-a review,, Industry Applications Conference, 1999. Thirty-Fourth IAS Annual Meeting. Conference Record of the 1999 IEEE, vol. 1, 1999, pp. 197–204.

[5] SCHOEN, R. R.—HABETLER, T. G.: Effects of Time-Varying Loads on Rotor Fault Detection in Induction Machines, Industry Applications, IEEE Transactions on **31** No. 4 (1995), 900–906.

[6] A Nonlinear Model of a Harmonic Drive Gear Transmission byTuttle, T.D.;Seering, W.P., Robotics and Automation, IEEE Transactions on **12** No. 3 (1996), 368–374, http://snake.robotics.olin.edu/harmonic_drive/tuttle_seering_96.pdf.

[7] Robust Torque Control of Harmonic Drive Systems byTaghirad, H.D., Citeseer, 1997, PhD dissertation http://saba.kntu.ac.ir/eecd/aras/papers/TR1-phd-thesis.pdf.

[8] HÄUPTLE, P.—HUBINSKÝ, P.—GRUHLER, G.—FELLHAUER, B.: Modellierung des Schwingungsverhaltens eines Mechatronischen Antriebes hinsichtlich dem Entwurf verschiedener Regelungstechniken – Internationales Forum für Mechatronik, IFM-ZHAW – Institut für Mechatronische Systeme, Winterthur, Swiss, Nov 2010.

[9] HÄUPTLE, P.—HUBINSKÝ, P.—GRUHLER, G.: Investigation to Gear-Box Disturbances in Mechatronic Drives, Proc. of the International Conference on Innovative Technologies in Bratislava, Slovakia, Sep 2011, pp. 432–435.

[10] SMITH, O. J. M.: Posicast Control of Damped Oscillatory Systems, Proceedings of the IRE **45** No. 9 (1957), 1249–1255.

[11] SINGER, N. C.—SEERING, W. P.: Using Acausal Shaping Techniques to Reduce Robot Vibration, Robotics and Automation, 1988. Proceedings., 1988 IEEE International Conference on, pp. 1434–1439.

[12] SINGHOSE, W.: Command Shaping for Flexible Systems: A Review of the First 50 Years, International Journal of Precision Engineering and Manufacturing **10** No. 4 (2009), 153–168.

[13] HUBINSKÝ, P.: Reducing of Robot End-Effector Residual Vibration by Means of Control Signal Shaping, J. Electrical Engineering **49** (1998), 129–133.

[14] HUBINSKÝ, P.—VRANKA, B.—JURIŠICA, L.: Genetic Algorithm Based Method of Elimination of Residual Oscillation in Mechatronic Systems, Kybernetika **41** No. 5 (2005), 623–636, http://dspace.dml.cz/bitstream/handle/10338.dmlcz/135682/Kybernetika_41-2005-5_5.pdf.

[15] HUBINSKÝ, P.—POSPIECH, T.: Slosh-Free Positioning of Containers with Liquids and Flexible Conveyor Belt, J. Electrical Engineering **61** No. 2 (2010), 65–74, http://iris.elf.stuba.sk/JEEEC/data/pdf/2_110-1.pdf.

[16] HÄUPTLE, P.—HUBINSKÝ, P.: Embedded Shaping Technique to Reduce Oscillations in Intelligent Drives, Proc. of the 6th South East European Doctoral Student Conference in Thessaloniki, Greece, Sep 2011, pp. 367–374.

[17] HÄUPTLE, P.—HUBINSKÝ, P.—GRUHLER, G.: Harmonic Modulation in Control to Reduce Oscillations in Mechatronic Systems, Proc. of the INES in Poprad, Slovakia, June 2011, pp. 303–308.

[18] HÄUPTLE, P.—HUBINSKÝ, P.—GRUHLER, G.: Harmonic Modulated Feedback in Control to Lower Oscillations in Mechatronic Systems,, Proc. of the 11th International Conference on Control, Automation and Systems in Gyeonggi-do/Seoul, Korea, =Oct 2011, pp. 273–276,.

[19] HUBINSKÝ, P. Rudolf,—B.—HÄUPTLE, P.: Optimization of the Signal-Type Used in a Harmonic Modulator for Control, Selected Topics in Modelling and Control. vol 7, FEI STU Bratislave, 2011.

[20] HÄUPTLE, P.—HUBINSKÝ, P.—RUDOLF, B.—GRUHLER, G.: Signal Types Investigation for Harmonic Modulation in Drives, Lecture Notes in Engineering and Computer Science: Proceedings of The World Congress on Engineering and Computer Science 2011, WCECS 2011, USA, vol. 2, Oct 2011, pp. 951–955, http://www.iaeng.org/publication/WCECS2011/WCECS2011_pp951-955.pdf.

[21] LUTZ, H.—WENDT, W.: Taschenbuch der Regelungstechnik, Deutsch Harri GmbH, 2010.

[22] DORF, R. C.—BISHOP, R. H.: Moderne Regelungssysteme, Pearson Studium, Aug 2007.

[23] Taschenbuch der Mathematik, 7th ed., Deutsch (Harri) byBronstein, I.N.; Semendjajew, K.A.;Musiol, G.;Muehlig,H., July 2008.

[24] MIČEK, J.—JURÍČEK, J.: Design of Multimode Shaper of Control Signals and Proper Choice of Sampling Frequency, The Canadian Journal on Automation, Control & Intelligent Systems **2** No. 3 (Apr 2011), 46–50, http://www.ampublisher.com/April%202011/ACIS-1104-011DesignofMultimodeShaperofControlSignalsandProperChoiceofSamplingFrequency.pdf.

[25] KOVÁŘ, O.: Discrete Realization of Control Signals Shaper, Journal of Information, Control and Management Systems **8** No. 3 (Apr 2010), 217–226.

Received 4 October 2011

Peter Hubinský born in 1962, received the Engineer degree in technical cybernetics from the Faculty of Electrical Engineering of the Slovak University of Technology, Bratislava in 1985. In 1992 he received the PhD degree from the same University. He specialized further in system theory and drive technology and control of robotic systems and worked as an assistant at the Faculty of Electrical Engineering in this time. Since 1999 he has been Assoc. Professor at the Faculty of Electrical Engineering and Information Technology, Slovak University of Technology, Bratislava. In 2011 he became a a full Professor at the same Faculty. His research and lecture activities are in the areas of servo systems, theory of dynamical systems, motion control systems, robotics and automation.

Peter Häuptle born in 1980, received the Engineer degree in Electronics and Information-technology from Heilbronn University, Germany in 2006. Since 2006 he has been an external PhD-student at the Faculty of Electrical Engineering and Information Technology, Slovak University of Technology, Bratislava. He is also a part-time lecturer for the Faculty of mechanics and electronics at Heilbronn University. His research interests are control of servomechanisms, digital signal processing, technical informatics as well as embedded coding of PLCs and microcontrollers.